

Optimizing the Electrode Configuration of a Cylindrical Discharge-Type Fusion Device by Computational and Experimental Analysis

Kazuyuki NOBORIO, Yasushi YAMAMOTO¹⁾ and Satoshi KONISHI²⁾

Hydrogen Isotope Research Center, University of Toyama, Toyama 930–8555, Japan

¹⁾*Faculty of Engineering Science, Kansai University, Suita 564–8680, Japan*

²⁾*Institute of Advanced Energy, Kyoto University, Uji 611–0011, Japan*

(Received 26 May 2014 / Accepted 8 August 2014)

A new design of a cylindrical discharge-type fusion device is proposed to achieve the precise alignment of components and prevent abnormal discharges. Cylindrical insulators that act as parts of the vacuum boundary and fix the relative position between cathode and anodes were used. The configuration of the electrodes was optimized to maintain stable discharge at low pressures and high discharge voltages, which enhances the neutron yield. The optimization was performed via analysis of the electric field and ion movements by developing a 2D code, and the results were experimentally verified. The results show that grounding the anodes is better for stable discharge at lower pressures. The optimized combination of the anode height and cathode overhang is 3 cm and 1 cm, or 2 cm, respectively. The discharge characteristics and neutron production rate were then experimentally measured for the optimized configuration. The attained highest discharge voltage (instantaneous) was ~50 kV and the neutron production rate of 3×10^4 n/s was obtained by continuous discharge with an applied voltage of 30 kV and discharge current of 30 mA.

© 2014 The Japan Society of Plasma Science and Nuclear Fusion Research

Keywords: discharge-type fusion device, neutron source, glow discharge, high voltage, IECF

DOI: 10.1585/pfr.9.1306142

The discharge-type fusion device has been developed as a compact on-site neutron generator based on research on inertial electrostatic confinement fusion (IECF). The spherical IECF device consists of a spherical chamber, which acts as the ground electrode (anode), and a grid cathode located in the center of the chamber [1–3]. By applying a high voltage (~100 kV) between the electrodes after loading with low-pressure (< 10 Pa) deuterium gas, a glow discharge is induced. The generated ions are accelerated toward the center of the cathode by the electric field, but most of them pass through the cathode because of its highly transparent shape. Therefore, they circulate in the chamber. This contributes to the generation of new pairs of ions and electrons via ionization, resulting in discharge at lower pressures relative to the solid cathode [4]. The low-pressure operation is considered effective for achieving higher neutron yield owing to the discharge characteristic of such devices (lower pressure makes the discharge voltage higher) and the cross section vs energy curve for the D–D fusion reaction. Furthermore, energy loss through reactions with background gas, such as charge-exchange, is expected to decrease with decreasing pressure. [4–6]

The original concept of IECF assumes fusion reaction owing to head-on collision among the accelerated ions in-

side the cathode, which is called “beam–beam reaction.” However, previous research revealed that the majority of neutron generation originates from collisions of the accelerated ions with the background neutral gas (called “beam–background reaction”) and that the reaction rate decreases with decreasing pressure, which is equivalent to decreasing the background target. [7–9].

We focused on another mechanism of fusion reaction, induced by energetic particles colliding with absorbed deuterium on the surface of the electrodes. We have tried to increase the reaction rate by coating the electrodes with hydrogen absorption materials such as titanium [9]. This concept is being developed as a neutron “beam” generator by using a cylindrical variation with reflectors and moderators [10–12]. However, the existing experimental machine, consisting of a grounded chamber and negatively biased cathode, has some problems; namely, unstable and inaccurate cathode support, undesirable discharge between the cathode and chamber wall, and overheating of the cathode after long operation.

We have proposed a new design where two electric insulators serve as the positioning spacers, as shown in Fig. 1. By using this design, which does not require the grounded chamber, it is possible to apply positive voltage to the anodes and keep the cathode grounded (C-GND) instead of the anode (A-GND). These drastic design changes

author's e-mail: noborio@ctg.u-toyama.ac.jp

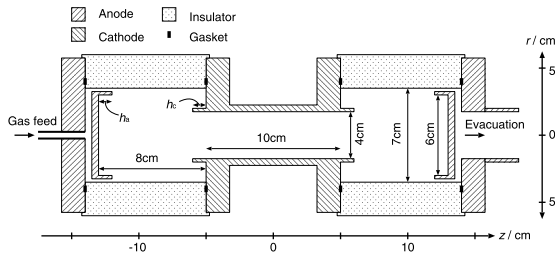


Fig. 1 Cross sectional sketch of the proposed fusion device with cylindrical insulators. The insulators are fixed between the anodes and cathode.

should cause large changes in the discharge characteristics; therefore, it is necessary to understand it and to optimize the electrodes configuration. In this study, the ground connection and electrode configuration (cathode overhang from its flange and anode rim height) were optimized by numerically analyzing the electric field and ion movement, and then experimentally verifying the results. In addition, the discharge characteristics and neutron production rate were investigated for the optimized electrodes configuration.

To analyze the ion movement in the device, a simple calculation program was developed. The electrostatic field is solved using the two-dimensional finite-element method (FEM) (cylindrical geometry). The contribution of the space charge was not considered because the plasma density is sufficiently small. The position and velocity of ions (D_2^+ : charge/mass = $1.60 \times 10^{-19} \text{ C} / 6.64 \times 10^{-27} \text{ kg}$) accelerated by the electric field was analyzed and traced. The geometrical parameters used in the calculations are noted in Fig. 1. The relative permittivity of the polytetrafluoroethylene (PTFE) insulator was taken at 2.1. The calculation limits were $-0.3 \text{ m} < z < 0.3 \text{ m}$ and $r < 0.3 \text{ m}$, and the boundary was assumed grounded. This also reflects the experimental conditions, in which grounded lead plates are located as X-ray shields at the same position as the calculation boundary. The applied voltage was 20 kV for the C-GND case or -20 kV for the A-GND case; however, the ion trajectories depend not on this value but on the shape of the potential.

By using this calculation code, the differences in the potential distribution and ion trajectories by changing the grounded electrodes and the geometrical configuration were investigated. Then, the electrode configuration was optimized to maintain stable discharge at lower pressures. Because the direct simulation of self-maintaining discharge had not been attempted, the flight path length of each ion was evaluated to determine suitable conditions lower pressure operation. In this method, virtual ions initially assumed 18 given positions with zero initial velocity, and the movement of each ion owing to the electrostatic field was traced until it collided with the structural objects (cathode or insulator) and the path length was recorded.

Increasing the path length increases the ionization induced by the ions during their flight. This makes discharge possible at lower pressures. However, not all traced ions reflect real discharge, and they are not considered in the evaluation because the initial positions are arbitrary. Therefore, only the ion with the longest recorded path length was selected for each condition, and the length characterizes the condition. Thus, the background gas is ionized in a limited region on that ion's path. This is reasonable considering that the "discharge path" is observed in the experiments. The interval of each initial position of ions (1 cm in the radial direction and 2 cm in the axial direction) was sufficiently fine compared with the discharge path.

Two cylindrical insulators were inserted between the anodes and cathode, as shown in Fig. 1. The insulators and cathode also serve as vacuum boundaries. By using Viton gaskets, a base pressure of 10^{-5} Pa was achieved. Gas feeding and evacuation systems, high voltage regulated power supply, and a neutron-measuring system with a ^3He proportional counter and polyethylene moderator were also included.

In contrast to the calculations, we could directly measure the discharge voltage and neutron production rate as a function of gas pressure and discharge current for each electrode condition. The gas pressure should be treated carefully because the ionization vacuum gauge (IVG) used in the experiment measures the gas density and displays it in units of pressure (Pa) assuming standard temperature. Furthermore, there was a temperature difference between the measuring point and the discharge area. Therefore, the actual gas density in the discharge chamber was estimated according to the following. The apparent total flow from the discharge chamber to the measuring point was negligibly smaller than the forward flow rate F_F (from the discharge chamber to the measuring point) and reverse flow rate F_R . Therefore, F_F and F_R are considered equivalent. Each flow rate is proportional to the product of the gas density and velocity at the source side, and the gas velocity is proportional to the square root of the temperature. Therefore, the gas density at the discharge area is expressed as

$$n_D = n_M \sqrt{\frac{T_M}{T_D}}, \quad (1)$$

where n and T , and subscripts D and M are the gas density and temperature, and discharge chamber, and measuring point, respectively. To measure the temperature of the discharge area, a thermocouple was attached to the backside of one of the anodes.

Figure 2 shows the ion trajectories with potential profiles of different grounding patterns. They differ depending on the grounded electrode. A divergent potential structure for ions is formed in the C-GND case and a convergent potential structure is formed in the A-GND case. This is supported by Fig. 3, which shows that the radial electric field $E_r (= -\partial\phi/\partial r)$ is positive (divergent for ions) for all z in the C-GND case and that E_r is negative (convergent for ions)

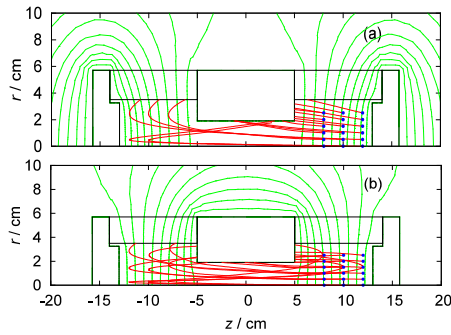


Fig. 2 Ion trajectories along with contour lines when (a) the cathode is grounded (C-GND) and (b) the anodes are grounded (A-GND). The latter gives more converging and longer ion trajectories.

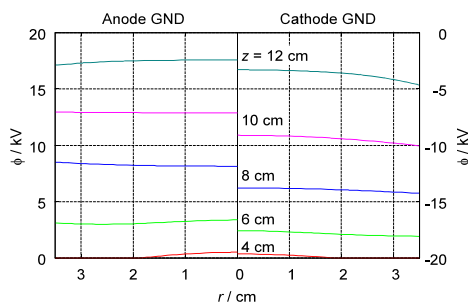


Fig. 3 Cross sectional potential profiles on the orthogonal plane to the z -axis for the two grounding patterns. The radial electric field ($E_r = \partial\phi/\partial r$) in the A-GND case is more divergent for the ions.

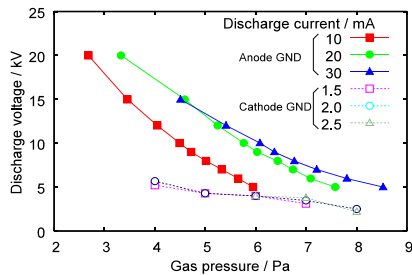


Fig. 4 Pressure and voltage characteristics for different discharge currents for A-GND and C-GND.

for $z = 8$ cm and $z = 10$ cm in the A-GND case. As a result, the maximal ion path length in the A-GND case (55 cm) is longer than that in the C-GND case (39 cm). This suggests that grounding the anodes is effective for maintaining the lower pressure discharge.

The experimentally observed pressure–voltage data for both grounding patterns and different discharge currents are shown in Fig. 4. The discharge voltage is not shown as a function of the gas density, however, is shown as a function of the gas pressure displayed in the IVG because the thermocouple had not been attached at this stage.

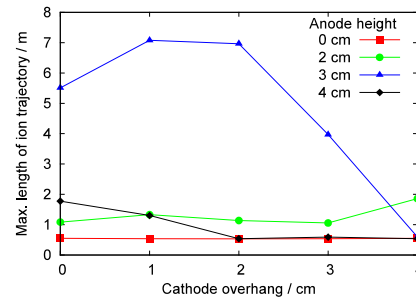


Fig. 5 Maximum path length of the ions in each cathode overhang and anode height.

Table 1 Maximum applied voltage and minimum gas pressure for each cathode overhang when the anode height is 3 cm.

Cathode overhang	Max. voltage	Min. pressure
1 cm	20 kV	2.7 Pa
2 cm	40 kV	2.6 Pa
3 cm	35 kV	3.9 Pa

At lower pressure, higher voltage, and larger current than those shown in Fig. 4, a sustainable discharge could not be observed (plasma disappeared or switched to abnormal discharge with a blinking flash). Lower pressure and higher current produce higher voltage, as shown in Fig. 4, which is common in other IECF devices. Grounding the anodes is effective for decreasing the lower limit of pressure and increasing the discharge voltage. This corresponds to the calculation results described above. By considering the computational and experimental results, grounding the anodes was evaluated.

The rim height of the anodes h_a and extension from the cathode flange h_c were the optimized parameters, and the other dimensions were fixed, as shown in Fig. 1. The calculated maximal ion path length for each electrode condition is shown in Fig. 5 and suggests that the most optimal combination of electrode geometry is $h_a = 3$ cm and $h_c = 1$ cm.

In the experimental verification, the anode height was fixed at 3 cm and cathode extensions of 1 cm, 2 cm, and 3 cm were tested because all combinations are difficult to be tested. Table 1 shows the highest discharge voltage and the lowest gas pressure available at each cathode condition when the discharge current was 10 mA. This experimental result suggests that the 2 cm cathode overhang is the best for discharge with higher voltage and lower pressure. This slightly differs from the calculation results of Fig. 5; however, the difference of 1 cm and 2 cm between the cathode overhangs is quite small in the calculations, the general trend agrees with the calculation results.

By using the optimized configuration of the electrodes, $h_a = 3$ cm and $h_c = 2$ cm, the discharge charac-

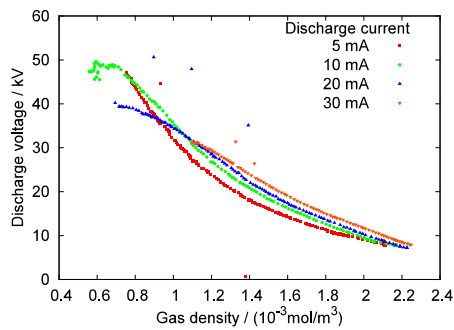


Fig. 6 Discharge voltage vs gas density. The gas density of 10^{-3} mol/m^3 is equivalent to 2.49 Pa when assuming a gas temperature of 300 K.

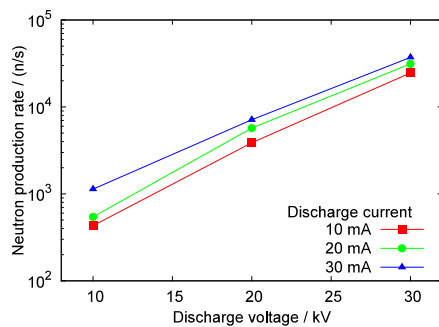


Fig. 7 Neutron production rate (NPR) as function of the discharge voltage at different discharge currents.

teristics and neutron production rate were measured experimentally. Figure 6 shows the discharge voltage as a function of the gas density estimated using Eq. (1) for different discharge currents. The discharge voltage suggests strong dependency on the gas density and weak dependency on the discharge current. This is reasonable compared with previously studied devices. The neutron production rate increases exponentially as a function of the discharge voltage, as shown in Fig. 7. This is due to the exponential increase of the cross section of the D–D fusion reaction corresponding to the ion energy. It may be curious that the maximum applicable voltage seen in Fig. 6 is 50 kV but there are no data on higher voltages than 30 kV in Fig. 7. This is because the plot in Fig. 6 shows instantaneous values, and the continuous discharge required for neutron counting (1 min) was only available at voltage lower than 30 kV.

Possible reasons for the instability of discharge at low pressure (gas density) were examined by analyzing the gas with a quadrupole mass spectrometer and observing the insulator after the discharge. The obtained mass spectra

showed some peaks at higher mass number, and the inner surface of the insulator indicated change in color (from white to brown) and cracks after the discharge. Hence, the instability presumably derives from the degradation of PTFE and degasification from the PTFE insulator owing to high temperature and particle bombardment during discharge.

In spite of the instability in this experiment, Fig. 7 shows exponential increase for the neutron production rate as a function of the voltage. If stable discharge with applied voltage of 60 kV becomes available, a neutron production of approximately $10^7/\text{s}$ is expected by extrapolation from Fig. 7. This will be realized using heat-resistant insulators.

In conclusion, a new design of cylindrical discharge-type fusion device was proposed, and the electrode configuration was optimized. By computationally tracking the ion trajectory and experimental measurements of the discharge characteristic, grounding the anodes with an anode height of 3 cm and a cathode overhang of 1 cm or 2 cm was the best configuration for discharge at lower pressure and higher voltage. This also proves that trajectory tracking can predict the availability of low-pressure discharge.

The measured discharge and neutron production rate for the optimized conditions were reasonable. However, higher voltage than 30 kV could not be applied because of degasification from the insulator. A neutron production rate of $10^7/\text{s}$ is expected by extrapolation if a voltage of 60 kV is applied.

Acknowledgments

The authors express their gratitude to Prof. Ryuta Kasada for his useful suggestions and to Mr. Yoshiyuki Nishinosono for his help with the experimental setup. This research was partly supported by JSPS KAKENHI 23760828.

- [1] R.L. Hirsch, *J. Appl. Phys.* **38**, 4522 (1967).
- [2] G.H. Miley *et al.*, *Proc. 3rd Int. Conf. Dense Z-pinchs*, AIP Press 675 (1994).
- [3] K. Yoshikawa *et al.*, *J. Plasma Fusion. Res.* **83**, 795 (2007).
- [4] G.H. Miley *et al.*, *IEEE Trans. Plasma. Sci.* **25**, 733 (1997).
- [5] C.R. Piefer *et al.*, *Fusion Sci. Technol.* **47**, 1255 (2005).
- [6] K. Masuda *et al.*, *Proc. 20th Symp. Fusion Eng.* 628 (2003).
- [7] K. Noborio *et al.*, *Fusion Sci. Technol.* **47**, 1280 (2005).
- [8] K. Noborio *et al.*, *Fusion Eng. Des.* **81**, 1701 (2006).
- [9] K. Noborio *et al.*, *Fusion Sci. Technol.* **52**, 1105 (2007).
- [10] T. Kanagae *et al.*, *Proc. 23rd Symp. Fusion Eng.* SP4B-47 (2009).
- [11] T. Maegawa *et al.*, *Proc. 24th Symp. Fusion Eng.* SP2-33 (2011).
- [12] N. Matsui *et al.*, *Fusion Sci. Technol.* **64**, 692 (2013).